University of Groningen

Systematics of inclusive photon production in 158 center dot A GeVPb induced reactions on Ni, Nb, and Pb targets

Aggarwal, MM; Agnihotri, A; Ahammed, Z; Angelis, ALS; Antonenko, [No Value]; Arefiev, [No Value]; Astakhov, [No Value]; Avdeitchikov, [No Value]; Awes, TC; Baba, PVKS

IMPORTANT NOTE: You are advised to consult the publisher's version (publisher's PDF) if you wish to cite from it. Please check the document version below.

Document Version
Publisher's PDF, also known as Version of record

[Link to publication in University of Groningen/UMCG research database](#)

Systematics of inclusive photon production in 158 · A GeV Pb induced reactions on Ni, Nb, and Pb targets

WA98 Collaboration

M.M. Aggarwal [a], A. Agnihotri [b], Z. Ahammed [c], A.L.S. Angelis [d], V. Antonenko [e],
V. Arefiev [f], V. Astakhov [f], V. Avdeitchikov [f], T.C. Awes [g], P.V.K.S. Baba [h],
S.K. Badyal [h], A. Baldine [f], L. Barabach [f], C. Barlag [i], S. Bathe [i], B. Batiounia [f],
T. Bernier [j], K.B. Bhalla [b], V.S. Bhatia [a], C. Blume [i], R. Bock [k], E.-M. Bohne [i],
Z. Böröcz [i], D. Bucher [i], A. Buijs [l], H. Büsching [i], L. Carlen [m], V. Chalyshev [f],
S. Chattopadhyay [c], R. Cherbatchev [e], T. Chujo [n], A. Claussen [i], A.C. Das [c],
M.P. Decowski [r], V. Djordjadze [f], P. Donni [d], I. Doubovik [e], S. Dutt [h],
M.R. Dutta Majumdar [c], K. El Chenawi [m], S. Eliseev [o], K. Enosawa [n],
P. Foka [d], S. Fokin [e], V. Frolov [f], M.S. Ganti [c], S. Garpman [m], O. Gavrishchuk [f],
F.J.M. Geurts [l], T.K. Ghosh [p], R. Glasow [i], S.K. Gupta [b], B. Guskov [f],
H.Å. Gustafsson [m], H.H. Gutbrod [j], R. Higuchi [n], I. Hrivnacova [o], M. Ippolitov [e],
H. Kalechofsky [d], R. Kamermans [l], K.-H. Kampert [i], K. Karadjev [e], K. Karpio [q],
S. Kato [n], S. Kees [i], H. Kim [g], B.W. Kolb [k], I. Kosarev [f], I. Koutcheryaev [e],
T. Krümpel [i], A. Kugler [o], P. Kulinich [r], M. Kurata [n], K. Kurita [n], N. Kuzmin [f],
I. Langbein [k], A. Lebedev [e], Y.Y. Lee [k], H. Löhner [p], L. Luquin [j], D.P. Mahapatra [s],
V. Manko [e], M. Martin [d], A. Maximov [f], R. Mehdiyev [f], G. Mgebrichvili [e],
Y. Miake [n], D. Mikhalev [f], Md.F. Mir [h], G.C. Mishra [s], Y. Miyamoto [n],
D. Morrison [t], D.S. Mukhopadhyay [c], V. Myalkovski [f], H. Naef [d], B.K. Nandi [s],
S.K. Nayak [j], T.K. Nayak [c], S. Neumaier [k], A. Nianine [e], V. Nikitine [f],
S. Nikolaev [e], P. Nilsson [m], S. Nishimura [n], P. Nomokonov [f], J. Nystrand [m],
F.E. Obenshain [t], A. Oskarsson [m], I. Otterlund [m], M. Pachr [o], A. Parfenov [f],
S. Pavliouk [f], T. Peitzmann [i], V. Petracek [o], F. Plasil [g], W. Pinanaud [j],
M.L. Purschke [k], B. Raeven [l], J. Rak [o], R. Raniwala [b], S. Raniwala [b],
V.S. Ramamurthy [s], N.K. Rao [h], F. Retiere [j], K. Reygers [i], G. Roland [r],
L. Rosselet [d], I. Roufanov [f], C. Roy [j], J.M. Rubio [d], H. Sako [n], S.S. Sambyal [h],
R. Santo [i], S. Sato [n], H. Schlagheck [i], H.-R. Schmidt [k], G. Shabratova [f], T.H. Shah [h],
I. Sibiriak [e], T. Siemiarczuk [q], D. Silvermyr [m], B.C. Sinha [c], N. Slavine [f],

K. Söderström [m], N. Solomey [d], S.P. Sørensen [t], P. Stankus [g], G. Stefanek [q],
P. Steinberg [r], E. Stenlund [m], D. Stüken [i], M. Sumbera [o], T. Svensson [m],
M.D. Trivedi [c], A. Tsvetkov [e], C. Twenhöfel [l], L. Tykarski [q], J. Urbahn [k],
N.v. Eijndhoven [l], G.J.v. Nieuwenhuizen [r], A. Vinogradov [e],
Y.P. Viyogi [c], A. Vodopianov [f], S. Vörös [d], B. Wysłouch [r],
K. Yagi [n], Y. Yokota [n], G.R. Young [g]

[a] *University of Panjab, Chandigarh 160014, India*
[b] *University of Rajasthan, Jaipur 302004, Rajasthan, India*
[c] *Variable Energy Cyclotron Centre, Calcutta 700064, India*
[d] *University of Geneva, CH-1211 Geneva 4, Switzerland*
[e] *RRC (Kurchatov Institute), RU-123182 Moscow, Russia*
[f] *Joint Institute for Nuclear Research, RU-141980 Dubna, Russia*
[g] *Oak Ridge National Laboratory, Oak Ridge, TN 37831-6372, USA*
[h] *University of Jammu, Jammu 180001, India*
[i] *University of Münster, D-48149 Münster, Germany*
[j] *SUBATECH, Ecole des Mines, Nantes, France*
[k] *Gesellschaft für Schwerionenforschung (GSI), D-64220 Darmstadt, Germany*
[l] *Universiteit Utrecht / NIKHEF, NL-3508 TA Utrecht, The Netherlands*
[m] *Lund University, SE-221 00 Lund, Sweden*
[n] *University of Tsukuba, Ibaraki 305, Japan*
[o] *Nuclear Physics Institute, CZ-250 68 Rez, Czech Republic*
[p] *KVI, University of Groningen, NL-9747 AA Groningen, The Netherlands*
[q] *Institute for Nuclear Studies, 00-681 Warsaw, Poland*
[r] *MIT Cambridge, MA 02139, USA*
[s] *Institute of Physics, 751-005 Bhubaneswar, India*
[t] *University of Tennessee, Knoxville, TN 37966, USA*

Abstract

The multiplicity of inclusive photons has been measured on an event-by-event basis for $158 \cdot A$ GeV Pb induced reactions on Ni, Nb, and Pb targets. The systematics of the pseudorapidity densities at midrapidity (ρ_{max}) and the width of the pseudorapidity distributions have been studied for varying centralities for these collisions. A power law fit to the photon yield as a function of the number of participating nucleons gives a value of 1.12 ± 0.03 for the exponent. The mean transverse momentum, $\langle p_T \rangle$, of photons determined from the ratio of the measured electromagnetic transverse energy and photon multiplicity, remains almost constant with increasing ρ_{max}. Results are compared with model predictions. © 1999 Published by Elsevier Science B.V. All rights reserved.

1. Introduction

The primary goal of ultra-relativistic heavy ion experiments is to study nuclear matter under extreme conditions, in which hadronic matter is expected to undergo a phase transition to a new state of matter, the Quark-Gluon-Plasma (QGP). For a thermalized system undergoing a phase transition, the variation of the temperature with entropy density is interesting as the temperature is expected to increase while below the transition, remain constant during the transition, and then increase again [1,2]. Temperature

fluctuations have also been proposed as a signature of the existence of a tricritical point in QCD [3]. These behaviours can be studied by two experimentally measured quantities, viz., the mean transverse momentum, $\langle p_T \rangle$, and the pseudorapidity density at midrapidity, ρ_{max}, for varying impact parameter, or centrality, for a number of colliding systems. These variables also provide additional information to characterize the evolving system. ρ_{max} provides a measure of the energy density which is important to understand the reaction dynamics [4,5]. In addition, the change in shape of the pseudorapidity distribution should be investigated in detail because it may provide a clue to the formation of the QGP phase [6,7].

Except for a few measurements of photon [8–11] and neutral meson [12–15] distributions reported earlier, most studies have been restricted to charged particle measurements (a review of charged particle measurements can be found in Ref. [16,17]), due to the difficulty of precise measurements of photon distributions. The inclusive photons provide a picture of the system at freezeout since the majority of the photons emitted from the reaction are decay products of produced particles, viz., π_0 and η_0, (only a small fraction is emitted directly during the initial stage of the collision [18]). The shape and width of the pseudorapidity distributions of photons may be different compared to those of the charged particles. Photon multiplicity measurements have also become increasingly important because of the recent interest in simultaneous measurements of the multiplicity of photons and charged particles in the search for Disoriented Chiral Condensates (DCC) [19,20]. The formation of a DCC is expected to give rise to large fluctuations in the relative number of emitted charged particles and photons, analogous to the Centauro and the anti-Centauro types of events observed in cosmic ray experiments [21]. Photon measurements can also be used to study flow [22] and intermittency behavior of events accompanying a possible phase transition.

In this letter, we present the first measurement of the photon multiplicity and pseudorapidity distributions, together with the $\langle p_T \rangle$ of photons produced in collisions of $158 \cdot A$ GeV Pb with Ni, Nb, and Pb targets, carried out in the WA98 experiment [23] at the CERN-SPS.

2. Experimental setup

In the WA98 experiment, the main emphasis has been on high precision, simultaneous detection of both hadrons and photons. The experimental setup consists of large acceptance hadron and photon spectrometers, detectors for charged particle and photon multiplicity measurements, and calorimeters for transverse and forward energy measurements. The present analysis makes use of the photon multiplicity detector (PMD), the midrapidity calorimeter (MIRAC) and the zero degree calorimeter (ZDC).

The PMD was placed at a distance of 21.5 meters from the target. It was a preshower detector consisting of 3 radiation length (X_0) thick lead converter plates in front of an array of square scintillator pads of four sizes, varying from 15×15 mm^2 to 25×25 mm^2, placed in 28 box modules. Each box module consisted of a matrix of 38×50 pads and was read out using one image intensifier $+$ CCD camera system. The scintillation light was transmitted to the readout device by using a short wavelength shifting fiber spliced with a long EMA (extra-mural absorber) coated clear fiber. The total light amplification of the readout system was $\sim 40\,000$. Digitization of the CCD pixel charge was done by a set of custom built fastbus modules employing an 8 bit 20 MHz Flash ADC system. Details of the design and characteristics of the PMD may be found in Ref. [24]. The results presented here make use of the data from the central 22 box modules covering the pseudorapidity range of $2.9 \leq \eta \leq 4.2$.

The MIRAC [25] was placed behind the PMD at 24.7 meters from the target. It consisted of 30 stacks, each divided vertically into 6 towers, each of size 20×20 cm^2, and segmented longitudinally into electromagnetic (EM) and hadronic sections. The depth of an EM section is $15.6\,X_0$ (equivalent to 51% of an interaction length) which ensures essentially complete containment of the electromagnetic energy, with 97.4% and 91.0% containment calculated for 1 GeV and 30 GeV photons, respectively. Hadrons also deposit a sizable fraction of their energy in the EM section. The MIRAC measures both the transverse electromagnetic (E_T^{em}) and hadronic (E_T^{had}) energies in the interval $3.5 \leq \eta \leq 5.5$ with a resolution of $17.9\% / \sqrt{E}$ and $46.1\% / \sqrt{E}$, respectively, where E is expressed in GeV. The ZDC measures the total

forward energy, E_F, with a resolution of $80\%/\sqrt{E}$ + 1.5%, where E is expressed in GeV.

3. Data analysis

3.1. Event selection

The data were taken during the December 1996 Pb beam period at the CERN SPS. The thicknesses of the three targets were 250 μm, 254 μm, and 213 μm for Ni, Nb, and Pb, respectively. The fundamental ''beam'' trigger condition consisted of a signal in a gas Čerenkov start counter located 3.5 meters upstream of the target and no coincident signal in a veto counter with a 3 mm diameter circular hole located 2.7 meters upstream of the target. A beam trigger was considered to be a minimum-bias interaction if the transverse energy sum in the full MIRAC acceptance exceeded a low threshold. The data were taken using an average beam intensity of 200–300 kHz during a 3.5s spill, the number of events recorded per spill being 150–200.

Beam pile up, where a second beam trigger occurs at a time when the detectors are integrating their signals from the triggered event, was rejected by (a) using the timing information from the trigger detectors, and (b) requiring that the sum of energies in the ZDC and the MIRAC were within 3σ from the mean of the distribution. Downstream interactions were also rejected by requiring a coincident signal from the forward hemisphere of the Plastic Ball detector which surrounded the target. To correct for other sources of background, data were also taken with no target in place.

The CCD readout of the PMD was cleared every 10 μs using a clear pulse of 1 μs width generated every 10 μs. This ensured that there was no substantial noise buildup on the CCD pixels between successive event triggers. A gate of 2 μs around the clear pulse was used to veto partially or fully cleared events. The clear clock operated asynchronously and was vetoed with a 5.6 ms wide pulse when a valid trigger occurred to allow complete readout of all pixels. A further check on possible pileup in the CCD cameras was made by using a 10 μs range TDC to measure the time difference between the arrival of the last clear clock and any valid event trigger. Events with multiple interactions within the 10 μs between clear pulses were rejected in the offline analysis.

The centrality of the interaction is determined by the total transverse energy measured in the MIRAC. For the $\langle p_T \rangle$ analysis, which used the MIRAC data directly, the centrality was determined instead by the forward energy, E_F, measured in the ZDC. The centralities are expressed as fractions of the minimum bias cross section as a function of the measured total transverse energy or measured E_F. The most central selection corresponds to the top 5% of the minimum bias cross section and the peripheral selection corresponds to the lower 50–80% range. Extreme peripheral events in the 80–100% range were not analyzed.

3.2. Data reduction in the PMD

The digitized pixel charges are processed by using a pixel-to-fiber map to form fiber signals corresponding to each scintillator pad. The signals from several neighbouring scintillator pads are combined to form clusters, characterized by the total ADC content and the hit positions. On average, there is a 92% probability for photons to shower in the lead converter and produce large signals. Compared to this, hadrons give a signal mostly corresponding to minimum ionizing particles (MIP). The majority of the hadrons are rejected by applying a suitable threshold on the cluster signal. A fraction of hadrons undergoing interaction in the lead converter produce signals larger than the threshold and appear as contaminants in the photon sample. The number of clusters remaining above the hadron rejection threshold is termed as γ-*like*. The characteristics of the preshower PMD are described by the following two quantities [24]:

$$\epsilon_\gamma = N_{cls}^{\gamma,th}/N_\gamma^{inc} \tag{1}$$

$$f_p = N_{cls}^{\gamma,th}/N_{\gamma\text{-like}} \tag{2}$$

where ϵ_γ is the photon counting efficiency and f_p is the fractional purity of the photon sample. N_γ^{inc} is the number of incident photons on the PMD and $N_{cls}^{\gamma,th}$ is the number of photon clusters above the threshold. Both ϵ_γ and f_p are determined by a

detailed Monte Carlo simulation using the VENUS 4.12 [27] event generator with default parameter settings and the detector simulation package, GEANT 3.21 [28]. The details of the simulation can be found in Ref. [24]. No lower threshold on the energy spectrum of photons is applied in the simulation. The photon counting efficiency decreases with increasing hadron rejection threshold. The purity improves significantly with increasing threshold only up to ~ 3 MIPs and then rather slowly at higher thresholds. For practical purposes a 3 MIP threshold appears as an optimum choice for hadron rejection. With this value the photon counting efficiencies for the central and peripheral cases are 68% and 73%, respectively. The purity of the photon sample in the two cases are 65% and 54%, respectively.

From the experimental data one determines $N_{\gamma\text{-like}}$, the number of clusters above the hadron rejection threshold. Using the estimated values of ϵ_γ and f_p, one obtains the number of photons incident on the detector in the event from the relation:

$$N_\gamma = N_{\gamma\text{-like}} \cdot f_p / \epsilon_\gamma \tag{3}$$

3.3. Extraction of $\langle p_T \rangle$ of photons

In a given event, the average transverse momentum of the produced photons may be expressed as

$$\langle p_T \rangle = \frac{E_T^{\text{em}}}{N_\gamma} \tag{4}$$

where E_T^{em} is the transverse component of the electromagnetic energy, and N_γ is the number of photons in a given η-region. In the WA98 experiment, E_T^{em} and N_γ are measured with the MIRAC and the PMD, respectively, on an event-by-event basis. These detectors have complete overlap in azimuth in the pseudorapidity region $3.5 \leq \eta \leq 4.0$. Hence the data in this region are used for computing the $\langle p_T \rangle$ using the above equation.

In order to obtain the final E_T^{em} for Eq. (4), the measured electromagnetic energy in the MIRAC towers must be corrected for (1) the hadronic contribution to the EM section of the MIRAC, and (2) the energy deposited in the lead converter of the PMD

because of its position in front of the MIRAC. The final expression may be written as:

$$E_T^{\text{em}} = \frac{\sum\limits_{i=1}^{N} \left[E_i^{\text{em}} - f_h \cdot f_{\text{bal}} \cdot \left\{ E_i^{\text{had}} / (1 - f_h) \right\} \right] \sin\theta_i}{1 - f_{\text{PMD}}} \tag{5}$$

where E_i^{em} and E_i^{had} are the energies measured in the electromagnetic and hadronic sections of the MIRAC towers, f_h is the fraction of the hadronic energy deposited in the EM section, f_{bal} is the balance factor taking into account the different responses for electromagnetic and hadronic particles in the EM section [25], N is the number of towers in the MIRAC within the given η range, θ_i is the polar angle of the ith tower, and f_{PMD} is the fraction of the electromagnetic energy deposited in the lead converter of the PMD. By combining results from the test beam data and simulation, the value of f_{PMD} has been found to be 15%. Details of the determination of f_{PMD} and other corrections are similar to those of Ref. [9].

3.4. Systematic errors

Several different sources contribute to the final systematic error in the determination of the number of photons, N_γ. The error due to the effect of clustering of the pad signals is the dominant one. This error is determined from the simulation by comparing the number of known tracks on the PMD with the total number of clusters obtained after clustering. Apart from the effect of multiplicity as discussed in Ref. [10], the arrangement of box modules in the present setup leads to splitting of clusters at the box boundaries. The net result is that the number of clusters exceeds the number of tracks with a deviation of 3% in the case of peripheral events and 7% for high multiplicity central events.

The number of γ-like clusters depends on the ADC value of the MIP peak as determined from Pb + Pb data. It has been estimated [24] that because of an admixture of $\sim 20\%$ photons in the MIP data sample, the extracted MIP ADC value is higher by 2 ADC channels. This causes the extracted photon multiplicity to be lower by 2.5%. We have included

this as a source of systematic error. The error on ϵ_γ because of the variation in pad-to-pad gains is found to be less than 1%.

The purity factor, f_p, depends on the ratio between the number of photons and charged particles within the PMD coverage. The systematic error associated with this ratio has been studied by using the FRITIOF [29] event generator in addition to VENUS. The average photon multiplicity estimated using FRITIOF is found to be higher by about 4% in peripheral and by 1% in central collisions, relative to the values obtained with VENUS.

The combined systematic error on the final photon multiplicity is asymmetric and varies with the centrality of the reaction. The total systematic errors are -3.4% and $+7.5\%$ for peripheral collisions and -7.1% and $+3.4\%$ for central collisions, varying little throughout the PMD acceptance. The negative error implies overestimation of the number of photons.

The photon counting efficiency determined in the present case relies on the energy spectra of photons as given by the VENUS event generator. As the conversion probability for low energy photons falls sharply [26] with decreasing energy below 500 MeV, the estimate of ϵ_γ may be affected if the energy spectra in the actual case is different. Preliminary measurements of the photon energy spectra with the WA98 lead glass spectrometer indicate that there is an enhancement of photons below $p_T = 250$ MeV/c over that given by VENUS. Taking into account this excess of low energy photons in the PMD acceptance, the photon counting efficiency would be overestimated by 2–9% for central events and 3–13% for peripheral events, the smaller value being for large pseudorapidity and the larger value being for the smaller pseudorapidity region of the PMD acceptance. This effect would increase the quoted PMD photon multiplicities. However, this uncertainty in the photon counting efficiency due to the uncertainty in the photon spectrum has not been included in the final errors presented in this letter. The WA98 low energy photon measurements will be described in a separate publication.

The systematic error on the determination of $\langle p_T \rangle$ depends on the error in both E_T^{em} and N_γ. The major source of errors in E_T^{em} are the contributions of hadronic energy deposited in the electromagnetic

section of the MIRAC and the fraction of the electromagnetic energy deposited in the lead converter of the PMD. This is estimated to vary from 8.8% to 10.5% from peripheral to central events. Thus the combined systematic error on $\langle p_T \rangle$ has been estimated to vary from 11.5% to 12.7%.

4. Results and discussions

The photon multiplicity is determined using Eq. (3) on an event-by-event basis from the total number of γ-like clusters within the PMD coverage. The target out contribution to N_γ is almost absent because of the 3 MIP threshold for hadron rejection. The resulting minimum bias distributions of N_γ are shown in Fig. 1 for Pb + Ni, Pb + Nb, and Pb + Pb reactions at $158 \cdot A$ GeV. For comparison, the corresponding photon multiplicity distributions from the VENUS 4.12 event generator with default parameter settings, are superimposed in the same figure. The shape of these three distributions is governed by the collision geometry. For asymmetric collisions of Nb and Ni targets, small shoulders are present around N_γ of 300 and 200, respectively. This shoulder is produced when a decrease in the impact parameter leads to little increase in particle production and the cross sections for these small impact parameters pile up at
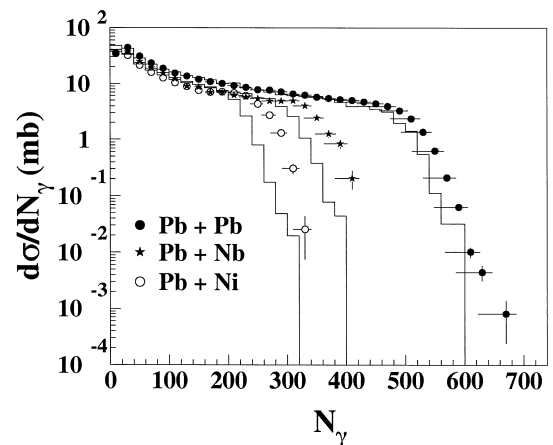

Fig. 1. Minimum bias inclusive photon cross sections for Pb + Ni, Pb + Nb, and Pb + Pb reactions at $158 \cdot A$ GeV. Solid histograms are the corresponding distributions obtained from the VENUS event generator.

a fixed N_γ. The VENUS event generator does not reproduce this shoulder well. The N_γ values are higher for the data compared to those of VENUS.

The pseudorapidity distribution of photons at different centralities are shown in Fig. 2 (a) for Pb + Pb collisions. The data have been corrected for geometry, efficiency, and purity factors. The filled symbols represent the measured data, and the open symbols are reflections of the filled symbols at $\eta_{c.m.}(= 2.92)$. The histograms show the corresponding distributions obtained from the VENUS event generator. The discrepancy between the VENUS results and the data is about 10% for central collisions at midrapidity. The pseudorapidity distribution of photons at different centralities for Pb + Nb and Pb + Ni are shown in Fig. 2 (b) and (c), respectively. The discrepancies between the data and VENUS are larger for these reactions compared to that of Pb + Pb.

The pseudorapidity distributions have been fitted with Gaussian functions to extract the peak position of the distribution (η_{peak}), the pseudorapidity density (ρ_{max}), and the width (σ). The fits are good in all

Fig. 3. (a) Pseudorapidity density (ρ_{max}), (b) width of the pseudorapidity distributions (σ), and (c) integrated values of number of photons (N_γ^{tot}), as functions of the number of participant nucleons at different centrality bins for Pb induced reactions on Ni, Nb, and Pb targets at $158 \cdot A$ GeV. The solid line in (c) is a power-law fit to the data, which yields the value of the exponent, $\alpha = 1.12 \pm 0.03$.
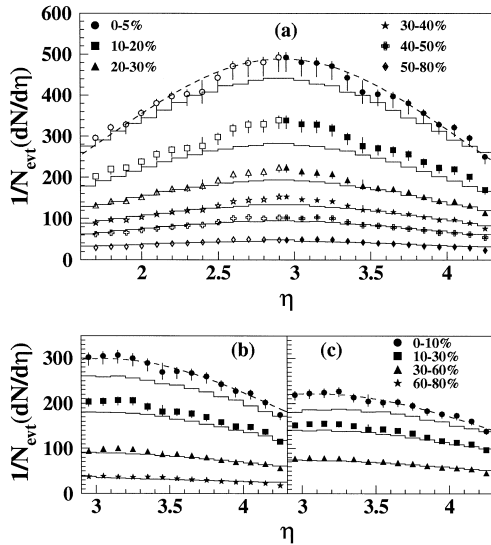

Fig. 2. Pseudorapidity distributions of photons in Pb induced reactions at $158 \cdot A$ GeV on (a) Pb, (b) Nb, and (c) Ni targets. The solid histograms are the corresponding distributions obtained from the VENUS event generator. In the Pb + Pb system, open symbols are the reflections of the measured data points around $\eta = 2.92$. The dashed curves represent gaussian fits to the data points corresponding to the case of 0–5% centrality for Pb + Pb and 0–10% centrality for Pb + Nb and Pb + Ni.
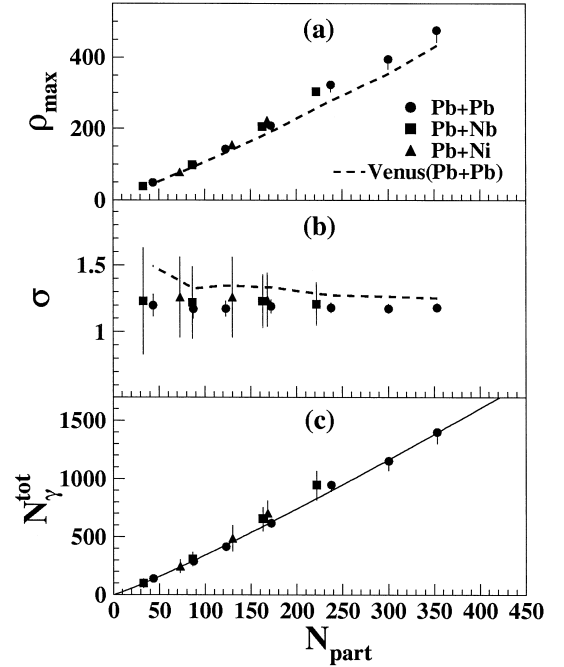
cases, χ^2 per degree of freedom being in the range of 2–4. Typical fits for the top centrality class for all the three targets are shown in Fig. 2. The η_{peak} values for Pb + Pb distributions remain constant at 2.92 for all centralities. For Pb + Nb, η_{peak} decreases from 3.03 ± 0.15 for central collisions to 2.95 ± 0.32 in the case of peripheral collisions. The corresponding values for the Pb + Ni reaction are 3.10 ± 0.16 and 2.99 ± 0.31. Fig. 3(a) and (b) show ρ_{max} and σ for the three reactions as functions of the number of participant nucleons, N_{part}, at different centralities. The N_{part} values are determined from the VENUS event generator. ρ_{max} increases with N_{part} while σ doesn't change with increase of N_{part}.

More insight into the systematics of the particle production can be obtained by computing the integrated number of photons (N_γ^{tot}) over the full phase space. This has been obtained from the Gaussian fit parameters to the pseudorapidity distributions.

Fig. 3(c) shows the extracted values of N_γ^{tot} for Pb + Pb as a function of N_{part}. The solid line shows a fit to the data using the function:

$$N_\gamma^{tot} = C \cdot \left(N_{part} \right)^\alpha \qquad (6)$$

where C is a proportionality constant. The value of the exponent, α, is extracted to be 1.12 ± 0.03. To further explore the systematics, we have divided the full η region (0–6) into two parts, one corresponding to the central rapidity region, $2.4 \leq \eta \leq 3.4$, and the other beyond this. For both of these cases, the Pb + Pb data yields a value of $\alpha = 1.12$. In comparison, fitting the photon distribution from the VENUS event generator in the same two regions yield different exponents, with 1.10 ± 0.07 at mid-rapidity and only 1.0 ± 0.05 for the outer region.

The mean transverse momentum, $\langle p_T \rangle$, as a function of ρ_{max}, the pseudorapidity density of photons at midrapidity, is shown in Fig. 4 for Pb + Pb collisions. For the data set considered, the target-out contributions were less than 1% for peripheral collisions and there was no effect for other centralities. The point at $\rho_{max} \simeq 525$ corresponds to the highest

centrality bin, 0–1% of the minimum bias cross section for Pb + Pb. The systematic errors on the absolute values are indicated by the upper and lower brackets on the figure. The $\langle p_T \rangle$ values are constant within the quoted error. For comparison, the results obtained from the VENUS event generator are superimposed in the figure. The $\langle p_T \rangle$ values obtained from VENUS are systematically higher compared to data, and show very little change with centrality. The indication of a small rise and saturation of $\langle p_T \rangle$ seen in the data is similar to what has been reported for neutral pions [15].

5. Summary

Photon multiplicities have been measured, on an event-by-event basis, in the forward region for $158 \cdot A$ GeV Pb induced reactions on Ni, Nb, and Pb targets. The peak positions of the photon pseudorapidity distributions are found to shift forward in going from the Pb target to Nb and Ni, as expected. The photon pseudorapidity densities increase with the number of participant nucleons, while the widths of the pseudorapidity distributions remain constant with centrality. The integrated number of photons scales like $N_{part}^{1.12}$, almost independent of the rapidity range over which the integration is performed. This is similar to the predictions of the VENUS event generator, except that VENUS shows a smaller power for forward rapidities. The photon mean transverse momentum has been determined from the event-by-event ratio of the electromagnetic transverse energy to the number of photons. After an initial rise with increasing ρ_{max}, the value of $\langle p_T \rangle$ is observed to remain constant.
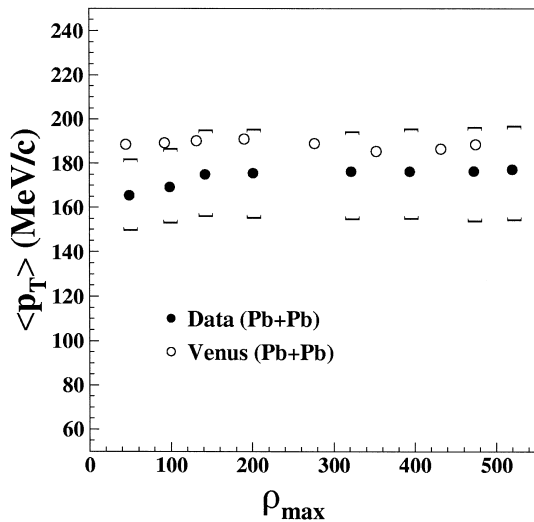
Acknowledgements

Fig. 4. The mean transverse momentum, $\langle p_T \rangle$, of photons as a function of the pseudorapidity density of photons at midrapidity, ρ_{max}, corresponding to different centralities. The $\langle p_T \rangle$ values obtained from the VENUS event generator for Pb + Pb are superimposed for comparison. Statistical errors on the data are within the size of the symbols and systematic errors are shown by the brackets.

References

[1] E.V. Shuryak, O. Zhirov, Phys. Lett. B 89 (1980) 253.

[2] L. van Hove, Phys. Lett. B 118 (1982) 138.

[3] M. Stephanov, K. Rajagopal, E. Shuryak, Phys. Rev. Lett. 81 (1998) 4816.

[4] J.D. Bjorken, Phys. Rev. D 27 (1983) 140.

[5] M. Kataja, P.V. Ruuskanen, L. McLerran, H. von Gersdorff, Phys. Rev. D 34 (1986) 2755.

[6] S. Sarkar, D.K. Srivastava, B. Sinha, Phys. Rev. C 51 (1995) 318; C 51 (1995) 2845 (E).

[7] A. Dumitru, U. Katscher, J.A. Maruhn, H. Stocker, W. Greiner, D.H. Rischke, Z. Phys. A 353 (1995) 187.

[8] WA93 Collaboration, M.M. Aggarwal, Phys. Rev. C 56 (1997) 1160.

[9] WA93 Collaboration, M.M. Aggarwal, Phys. Lett. B 404 (1997) 207.

[10] WA93 Collaboration, M.M. Aggarwal, Phys. Rev. C 58 (1998) 1146.

[11] WA80 Collaboration, R. Albrecht, Phys. Lett. B 201 (1987) 390.

[12] WA80 Collaboration, R. Albrecht, Nucl. Phys. A 488 (1988) 651.

[13] WA80 Collaboration, R. Albrecht, Phys. Lett. B 361 (1995) 14.

[14] WA80 Collaboration, R. Albrecht, Eur. Phys. J. C 5 (1998) 255.

[15] WA98 Collaboration, M.M. Aggarwal, Phys. Rev. Lett. 81 (1998) 4087.

[16] J. Stachel, G.R. Young, Ann. Rev. Nucl. Part. Sc. 44 (1994) 537.

[17] M.M. Aggarwal, S.I.A. Garpman, Int. J. Mod. Phys. E 4 (1995) 477.

[18] E.L. Feinberg, Nuovo Cimento A 34 (1976) 391; E.V. Shuryak, Phys. Lett. B 79 (1978) 135; B. Sinha, Phys. Lett. B 197 (1987) 263; D.K. Srivastava, B. Sinha, Phys. Rev. Lett. 73 (1994) 2421.

[19] J.D. Bjorken, K.L. Kowalski, C.C. Taylor, Baked Alaska, SLAC-PUB-6109, 1993 and hep-ph/9309235; K. Rajagopal, F. Wilczek, Nucl. Phys. B 399 (1993) 395.

[20] M.M. Aggarwal et al., WA98 Collaboration, Phys. Lett. B 420 (1998) 169; T.K. Nayak et al., WA98 Collaboration, Nucl. Phys. A 638 (1998) 249c.

[21] C.M.G. Lattes, Y. Fujimoto, S. Hasegawa, Phys. Rep. 65 (1980) 151; Y. Takahasi et al., JACEE Collaboration, in: L. Jones (Ed.), Proc. 7th Int'l. Symp. on Very High Energy Cosmic Ray Interactions, 1992, Ann Arbor, Michigan.

[22] WA93 Collaboration, M.M. Aggarwal, Phys. Lett. B 403 (1997) 390.

[23] Proposal for a Large Acceptance Hadron and Photon Spectrometer, CERN/SPSLC 91-17, SPSLC/P260.

[24] M.M. Aggarwal, Nucl. Instr. and Meth. A 424 (1999) 395.

[25] T.C. Awes, Nucl. Instr. and Meth. A 279 (1989) 479.

[26] M.M. Aggarwal, Nucl. Instr. and Meth. A 372 (1996) 143.

[27] K. Werner, Phys. Rep. C 232 (1993) 87.

[28] R. Brun et al., GEANT3 user's guide, CERN/DD/EE/84-1, 1984.

[29] B. Nilsson-Almqvist, E. Stenlund, Comp. Phys. Comm. 43 (1987) 387.